Photoactive Proton Conductor: Poly(4-vinyl pyridine) Gel

Naum Berestetsky,[†] Evgenia Vaganova,*[,†] Ellen Wachtel,[‡] Gregory Leitus,[‡] Alexander Goldberg,[§] and Shlomo Yitzchaik*[,†]

Department of Inorganic and Analytical Chemistry and the Farkas Center for Light-Induced Processes, The Hebrew University of Jerusalem, 91904, Jerusalem, Israel, Chemical Research Support Unit, Weizmann Institute of Science, 76100, Rehovot, Israel, and The Material Science Department, Accelrys, 92121, San Diego, California 92121

Received: November 20, 2007; In Final Form: January 7, 2008

We describe a hydrogen-bonded poly(4-vinyl pyridine)-based dielectric material, in which conductivity can be induced due to the presence of side-chain protonated species that form spontaneously when the polymer is dissolved in pyridine. The conductivity of the proton conductive gel can be controlled by direct irradiation at the proton-transfer center: a reversible change of conductivity was observed in response to the on/off switching of 385 nm wavelength radiation. Over most of the range of intensities used, the proton conductivity exhibited a bimolecular character. We present a model of the protonated pyridine side-chain unit in the ground and excited states (DFT level). In the ground state, the protonated pyridine moiety has a cyclic, conjugated structure.

Introduction

Conductivity in polymeric systems can include two components: electrical conductivity due to conjugation and ionic conductivity due to proton transfer.[1,2] One of the earliest excited-state proton-transfer studies was initiated to elucidate the interactions occurring in the excited state of hydrogen-bonded base pairs of DNA.[3] Biprotonic phototautomerism was found to occur in the 7-azaindole dimer (a model for base-paired DNA) in fluid solvents, but the phenomenon was not observed when the solvent was frozen.[3] Conductivity due to proton transfer may be controlled in a straightforward manner by both internal (e.g., addition of salts) as well as external factors such as irradiation.[4−6] Recently, examples of proton conductivity produced by the formation of hydrogen-bonded complexes of different strengths[7] and by doping the polymer system with a photoacid generator[8] have been presented. Study of excited-state proton transfer in some aromatic chromophores showed that some compounds (such as hydroxyarils and aromatic amines) increase their acidity in the excited state, whereas photobases (such as nitrogen heteroaromatics) increase their basicity.[9,10] Later, the design of a super photoacid—the strongest reversible photoacid—was presented.[11,12] Intramolecular proton transfer is possible when the acidic and basic moieties exist in proximity within the same molecule.[13,14] Interaction with the solvent molecules—excited-state proton transfer to the solvent—led to an intermolecular reaction.[15] Consideration of the elementary steps in excited-state proton transfer revealed that the intramolecular charge transfer to the ring system is more prominent for the anionic base than the acid. The charge redistribution triggers changes in hydrogen-bond strengths that set the stage for the proton transfer itself. This stage is very sensitive to the solvent, temperature, and adjacent molecules. Over longer times, the photoinduced proton may recombine adiabatically with the excited base or quench it.[15] In hydrogen-bonded systems, the dynamic properties of proton transfer are less studied, due to their complexity. Some examples are as follows: a theoretical study of proton transfer along hydrogen bonds,[16] proton motion in hydrogen-bonded quasi-1-D molecular chains,[17] and proton migration along a short hydrogen-bonded network in green fluorescent proteins.[18,19] The study of the proton transfer and hydrogen-bonding interactions in the stoichiometric pyridine−methanesulfonic acid complex was used as a model.[20] It was shown that the dielectric medium and the configuration of the complex have a pronounced effect on the hydrogen bond between an aromatic base and a strong acid.[20]

Of the polymers that are capable of forming proton conductive systems, one of the most frequently studied is poly(4-vinyl pyridine) (P4VPy).[5,21−26] The proton conductivity of linear chain, saturated P4VPy is due to the ability of the polymeric pyridine to form hydrogen-bonded complexes of different strengths. However, in most cases, the polymeric pyridine has been protonated synthetically (e.g., by the addition of Li salts or phosphoric acid or by functionalization of the pyridine ring).[22,24−26] In contrast, here we present a P4VPy-based system, in which the proton conductivity in the hydrogen-bonded system is due to side-chain protonated species, which form spontaneously when the polymer is dissolved in pyridine.[27] We show that the conductivity of the proton conductive system based on P4VPy can easily be controlled by direct irradiation at the proton-transfer center of the side-chain protonated species. In the P4VPy/Py gel, the close proximity of the two species, free pyridine molecules (photobase)[28] and the protonated polymeric pyridine molecules (photoacid)[11], makes the P4VPy/Py gel a suitable system for excited-state proton transfer. The polymeric gel displays a reversible change of conductivity in response to the on/off switching of 385 nm wavelength radiation. We demonstrate the proton and electron contributions to the photoinduced conductivity response and present a model of the

* Corresponding authors. Tel.: 972 2658 6971; fax: 972 2658 5319; e-mail: (E.V.) gv@cc.huji.ac.il and (S.Y.) sy@cc.huji.ac.il.
[†] The Hebrew University of Jerusalem.
[‡] Weizmann Institute of Science.
[§] Accelrys.

10.1021/jp711038u CCC: $40.75
Published on Web 03/05/2008

working species. We believe that the gel may prove to be useful as a practical, optical switching device.

Experimental Procedures

Materials. P4VPy, with a molecular weight of 50 000, was used (Polyscience, Inc.). The polymer was carefully dried in a vacuum oven (10^{-3} Torr) at 25 °C for 3−4 weeks before use. The pyridine was anhydrous (water <0.003%) and obtained from Aldrich. The molar ratio between polymer side-chain units and free pyridine molecules was 1:1. All procedures involving the initial viscous solution and gel preparation were accomplished in a glovebox under nitrogen atmosphere. The gelation of the P4VPy/Py viscous solution occurred spontaneously during the storage of the initial viscous solution for not less than 1 month. The stage of gelation was evaluated visually. For encapsulation, the prepared samples were kept in a glove box under nitrogen atmosphere for 5−6 h and then covered with Parafilm (Pechiney) to prevent solvent evaporation.

Spectroscopy. Excitation and photoluminescence (PL) spectra were measured on a Shimadzu RF-5301PC spectrofluorimeter. The data were collected at right angles to the excitation beam. The resolution of the emission and excitation spectra was 0.2 nm. Multiwavelength UV irradiation (at 385 ± 10 nm, intensity 5.3 mW/cm^2) was accomplished by a xenon short arc lamp (Ushio) inside the Shimadzu RF-5301PC. Fluorescence lifetime measurements were made by means of a FluoTime 200 (PicoQuant GmbH) instrument with a pulsed diode laser (PDL) 800-B, $\lambda = 410$ nm, pulse fwhm 54 ps, repetition frequency 40 MHz, peak power 219 mW. Data Analysis Software FluoFit (PicoQuant GmbH) was used for lifetime measurements. For pulse control, a solution of Ludox was used.

Conductivity. For the photoinduced conductivity measurements, the samples were prepared by sandwiching the polymer gel between indium-tin oxide (ITO) covered glass slides (SPI, Inc., 30−60 Ω) separated by 100 ± 5 μm or between an ITO covered glass slide and a Si/SiO_2 slide. Si/SiO_2 slides (Wafer World, Inc.) (oriented (100), resistance <1 Ω cm, *n*-type) were used. Photoinduced conductivity changes were measured with a multimeter (197 autoranging microvolt DMM, Keithley), which was used both as a source of the dc bias voltage and for performing the conductivity measurements. The multimeter controlled the value of the applied electric field (2 V). The external dc electric field induced the formation of an internal electric field due to the low dark ionic conductivity of the gel. The internal electric field, which exceeded 1 kV/cm, directed the photoinduced charge carriers produced by direct irradiation at the proton-transfer center.

Three temperature controlled cells were used (S.C.T. cell holder (Shimadzu) with TEP-1 immersion thermostat (Fried Electric), TCC controller (Shimadzu), and and tempcontrol 37 (Zeiss)) depending on the kind of measurement. Four-probe resistance measurements were carried out at room temperature using the Keithley switch system 7001, multimeter 2000, dc and ac current source 6221, picoameter 6485, and Stanford Research System Lock-In Amplifier SR830.[29]

Modeling. The Accelrys computer program with module DMol^3 (Accelrys) was used for modeling. All calculations reported in this paper were performed using DMol^3; all electron codes were based on the DFT calculations provided by Accelrys Inc.[30,31] A double numerical polarized (DNP) basis set was employed that included all occupied atomic orbitals plus a second set of valence atomic orbitals plus polarized d-valence orbitals.

For exchange and correlation, we applied a gradient-corrected approach using the generalized gradient approximation (GGA) functional in the manner suggested by Perdew−Burke−Ernzerhof (PBE).[32,33] The estimated error was found to be lower than that obtained with the hybrid B3LYP 6-31G** functional. The energies of formation obtained came within a factor of 2 in accuracy of the most accurate G2 DFT method. The spin unrestricted approach was applied with all electrons being considered explicitly. In all calculations, atom centered grids were used for numerical integration using approximately 2000 grid points for each atom. A real space cutoff of 3.7 Å was imposed. The self-consistent field (SCF) convergence criterion was set such that the root-mean-square (rms) change in the electronic density would be less than 1×10^{-6} Ha. Geometries were optimized using an efficient algorithm taking advantage of delocalized internal coordinates. The convergence criteria applied for geometry optimization were 1×10^{-5} Ha for energy, 0.002 Ha/Å for force, and 0.005 Å for displacement. For all the optimized structures, we performed a frequency analysis to check as to whether the structure obtained was a true minimum. In DMol^3, frequencies were evaluated by finite differences.

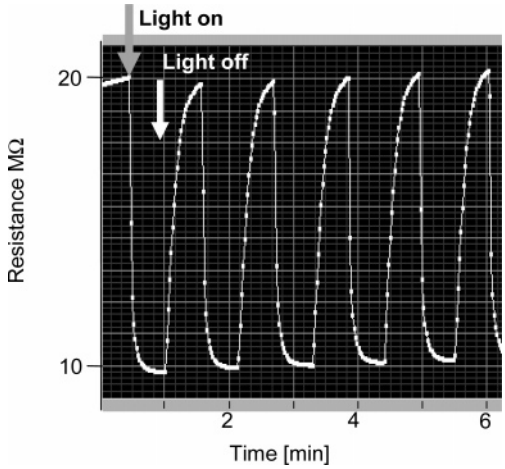

Figure 1. Periodic resistance changes of a 100 μm thick film of the P4VPy/Py gel (area 1 cm^2) placed between two glass/ITO electrodes. Irradiation at 385 nm was accomplished with a 5.3 mW/cm^2 xenon lamp. The internal dc electric field exceeded 1 kV/cm. The stabilized temperature of observation was 23.5 ± 0.1 °C.

Results

Photoinduced Conductivity. P4VPy spontaneously forms a gel when dissolved in pyridine and after being stored in the dark for 1 month. We measured the conductivity of the P4VPy/Py gel by using the four-point method with an alternating current in the frequency range of 100 Hz −to 1 kHz to prevent electrode polarization. The conductivity (σ) of the gel was measured to be 10^{-7} S/cm, indicating that, in principle, the P4VPy/Py gel is a dielectric. However, under irradiation at 385 nm, the dc resistance of the P4VPy/Py gel was reduced by as much as 50% from its initial value (Figure 1): from 18−20 MΩ to 9−10 MΩ. A steady value was achieved after ∼8−12 s of irradiation. The process is completely reversible, and we did not observe any fatigue of the effect following more than 150 cycles of the off/on switching sequence (data not shown). To evaluate the time scale of the processes, we investigated the resistance decay (R_t). We determined that, to a good approximation, the relaxation can be described as a double-exponential process

$$R_t = R_1 \exp(-(t - t_0)/\tau_1) + R_2 \exp(-(t - t_0)/\tau_2) + \text{constant} \quad (1)$$

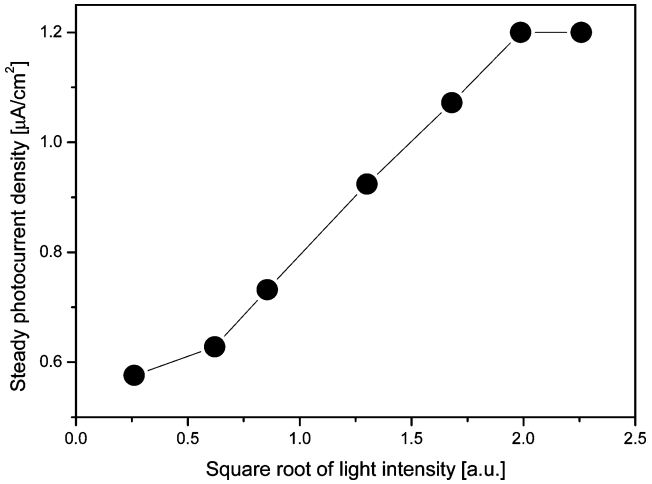

Figure 2. Dependence of the steady photocurrent density in Figure 1 on the square root of the light intensity.

where τ_1 and τ_2 are the time constants of the photochemical processes. Two different time scales were found: $\tau_1 = 0.60-0.70$ s and $\tau_2 = 2.40-3.36$ s (for the temperature range of 10−30 °C). Investigation of the spectral range of photoinduced conductivity showed that the photoresponse of the gel was maximal at 385 nm wavelength (data not shown). Figure 2 shows that for the P4VPy gel, the saturated photocurrent varied linearly with the square root of the intensity of the radiation over most of the measured range. This functional behavior is known to be characteristic of a bimolecular process[34] (i.e., a combination of independently generated charge carriers is responsible for the photoinduced current). However, at both low and high light intensities, a deviation from the square root dependency was observed. This indicated that there was a threshold in the low-intensity range and, most likely, a limit to the concentration of the excited centers in the P4VPy gel at high intensities. To elucidate the bimolecular character of the photocurrent and to separate the electron and proton contributions to the current, we measured the photoresistance changes when a Si/SiO_2 electrode was used instead of the second glass/ITO electrode. In the mixed electrode arrangement, the glass/ITO electrode was grounded. The data are presented in Figure 3. As can be seen, the back response that occurs in the dark was significantly faster (i.e., within 1 s (within the accuracy of our measurement) instead of ~30 s for the glass/ITO−glass/ITO electrode system). However, the photoresistance changes did not exceed 30% of those observed with the matched electrode arrangement.

Photoinduced Emission. We used the photoinduced light emission of the P4VPy/Py gel as a tool to investigate the nature of the photoexcited centers.[35] Figure 4 shows the emission spectra of the gel under excitation at wavelengths between 240 and 280 nm. Absorption at 250 nm (4.94 eV) is due to the $\pi-\pi^*$ transition;[36] absorption at 280 nm (4.41 eV) is clearly visible in the spectrum of the absorption of P4VPy in pyridine[37] and is assigned to the $n-\pi^*$ transition.[36] Excitation at 250 nm to the S_2 (π,π^*) state of pyridine produced dual emission with peaks at 370 and 385 nm. The mechanism of dual emission when pyridine is excited to the S_2 state was studied in detail by Pierola et al. for poly(2-vinyl pyridine) in a methanol/water solution.[38] They showed that the origin of the dual emission is the coexistence of pyridine side-chain units with different strengths of hydrogen bonding: emission at 350 nm was assigned to hydrogen-bonded species, and emission at 390 nm was assigned to protonated species.[38] The intensity of the emissions at 370 and 385 nm can be reversed if the gel is exposed to ammonium

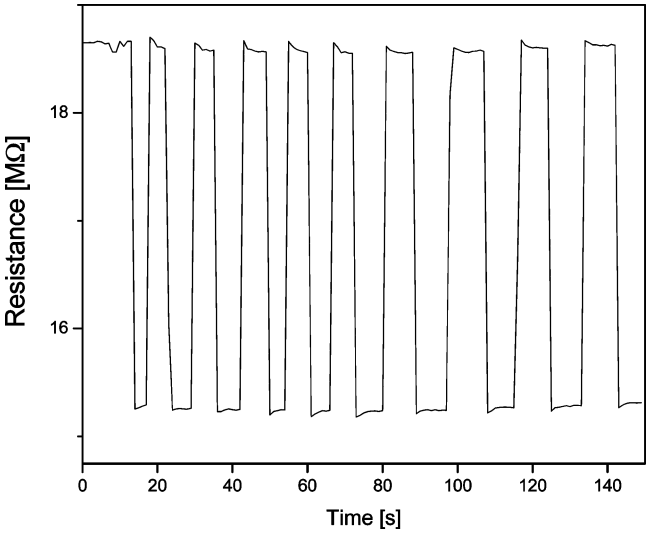

Figure 3. Periodic resistance changes of a 100 μm thick film of the P4VPy/Py gel (area 1 cm^2), placed between one glass/ITO electrode and one Si/SiO_2 electrode. Irradiation at 385 nm was accomplished with a 5.3 mW/cm^2 xenon lamp. The internal dc electric field exceeded 1 kV/cm. The stabilized temperature of observation was 23.5 ± 0.1 °C.

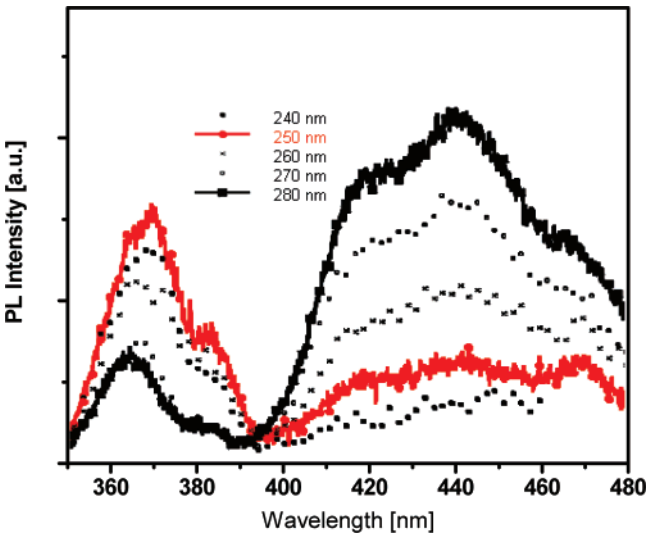

Figure 4. Emission spectra of the P4VPy/Py gel under excitation at wavelengths of 240 nm, 250 nm, 260 nm, 270 nm, and 280 nm.

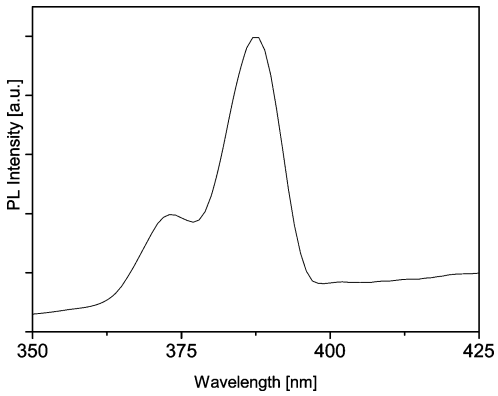

Figure 5. Emission spectrum of the P4VPy/Py gel, following exposure to NH_4OH (excitation at 250 nm).

hydroxide vapor (Figure 5). As shown in Figure 5, the intensity of the emission at 385 nm was significantly increased. We suggest that this intensity increase, which is linearly related to

the time of exposure, was due to the enhancement of the protonation of the polymeric pyridine moieties by the NH_4^+ groups of the ammonium hydroxide vapor. A similar effect was observed when the non-encapsulated gel was exposed to dry ammonia gas[39] (data not shown), thereby strengthening the identification of the protonating species.

Scanning the gel with excitation wavelengths between 260 and 460 nm revealed another important characteristic of the emitting center. The intensity of the emission at 370 nm decreased when we increased the excitation wavelength to 260 nm, 270 nm, and finally to 280 nm; the emission at 385 nm became practically undetectable. However, at the same time, a new broad and intense emission, centered at 440 nm and possessing structural features, appeared. Monitoring the gel emission as a function of longer excitation wavelengths from 370 to 460 nm indicated that the most intense emission at 440 nm was observed under excitation at 385 nm (quantum yield 0.18, data not shown). The time-resolved fluorescence of the emission at 440 nm, maximally excited at 385 nm, was well-fit by a triple exponential decay. The fast component (within the accuracy of our measurements) has a lifetime of 50 ps (84%), while the other two—with lifetimes of 1.1 and 4.8 ns—are less populated, 12 and 4%, respectively.

Discussion

Hydrogen Bonding. The ability to protonate is an intrinsic property of pyridine and therefore also of P4VPy. Our earlier FTIR investigation showed that two kinds of hydrogen bonding (primary and secondary) are responsible for minimizing the energy of the gel structure. The primary hydrogen bonds appear immediately after polymer dissolution in pyridine, forming N^+-H groups (H-bond energy of ~4−6 kJ/mol), and belong to the polymeric pyridine species.[27,40] These bonds can be associated with a vibrational band at 3400 cm^{-1}. The source of the protons has been identified as the CH group of the polymer backbone.[27] Preliminary NMR data also support this assignment (data not shown). A second type of hydrogen bond develops as the gelation progresses. The FTIR spectrum of the gel displayed a broad absorption at 1700 cm^{-1}, which is characteristic of quasi-symmetrical hydrogen bonding.[40] Quasi-symmetrical secondary hydrogen bonding has a strength of ~50 kJ/mol. The temporal behavior of this band may allow it to be associated with the progressive cross-linking in the gel.

In analogy to the work of Pierola et al.,[38] and also in view of the inverted fluorescence intensity in the gel protonated by ammonium (Figure 5), we made the following spectroscopic assignments. The emitting centers with emission at 370 nm (Figure 4) were identified as hydrogen-bonded species, and the emitting centers with emission at 385 nm were identified as polymeric protonated pyridine species. It is reasonable to conclude that not all polymeric pyridine side-chain units are hydrogen-bonded or protonated. The fact that the exposure of non-encapsulated samples of the gel to ammonium hydroxide vapor or dry ammonia gas succeeds in protonating additional side-chain units (Figure 5) supports this supposition. Nevertheless, at this stage, we are not able to estimate the amount of such working species.

The emission spectra (Figure 4) also provide us with information concerning the electronic conformation of the protonated center: it is electronically decoupled from the π,π^* states as there is no emission at 440 nm following excitation at 250 nm. The time-resolved fluorescence of the emission at 440 nm, excited at 385 nm, confirmed that a proton-transfer mechanism is involved in the excited-state deactivation. The fast component (50 ps) is typical of proton-transfer emission,[41] while the other two (1.1 and 4.8 ns)— are less populated. These can be assigned to the deactivation of the excited state of the N^+-H species, interacting with adjacent molecules, which points to the participation of non-radiative processes.[42,43]

SCHEME 1: Non-optimized Scheme of Poly(4-vinyl pyridine) Structure in the Gel

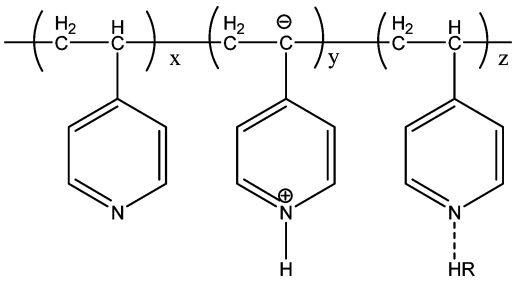

A non-optimized structure of the polymer in the gel is proposed in Scheme 1. On the basis of the existing results, we can describe the structure of the polymer in the gel as a mixture of at least three different kinds of side-chain moieties: regular pyridine side-chain units, fully protonated species with the transfer of the hydrogen from the CH group to the ring nitrogen, and hydrogen-bonded species, responsible for cross-linking in the gel.

Proton Transfer. Direct excitation at 385 nm of the protonated species in the P4VPy gel led to excited-state proton transfer. Evidence for proton transfer under irradiation at 385 nm includes a reversible pH decrease from 9.1 to 8.4[40] and a significant increase in gel conductivity (Figure 1). Therefore, we can identify the emitting center at 385 nm as the proton-transfer center and the excited state as the proton-transfer state. Three principal mechanisms may describe proton transfer: Grotthuss, vehicle,[4] and proton transfer in hydrogen-bonded media as pointed out in the early work of Eigen and De Mayer.[44] The Grotthuss mechanism is based on proton transfer via segmental motion, which involves the motion of groups of atoms on the polymer backbones. The rate of reorganization is usually relatively slow, thereby limiting the hopping rate, while the vehicle mechanism, which needs suitable coordination sites adjacent to the ions so that they may hop, is limited by the diffusion rate of the side chains. The slow process that we observed ($\tau_1 = 2.40-3.36$ s) may reflect the reorganization of the polymer backbone, while the more rapid process ($\tau_2 = 0.60-0.70$ s) may result from the contribution of the mobile pyridine molecules to proton hopping.[15] The role of the free pyridine molecules in determining the photoconductivity of the gel is currently under investigation. The square root dependence of the saturated photocurrent on the intensity of the irradiating light revealed a bimolecular character over most of the intensity range (Figure 2).

To calculate the proton mobility in the excited state of the gel, we considered the equation proposed by Petriz for the photoconductive response to irradiation[45]

$$\Delta\sigma = (1 + B)q\mu g\tau[1 + (\omega\tau)^2]^{1/2} \qquad (2)$$

where $\Delta\sigma$ is the conductivity change, q is the charge of the current carrier, μ is the carrier mobility, B is a parameter characterizing the relative effect of barrier modulation (no barrier modulation ($B = 0$) was used in the present calculation), g is the rate of absorption of the incident photons, τ is the lifetime of the charge carrier, and ω is the angular frequency of the on/

SCHEME 2: Modeling (DFT Level) of the Structure of the Protonated Polymer Moiety

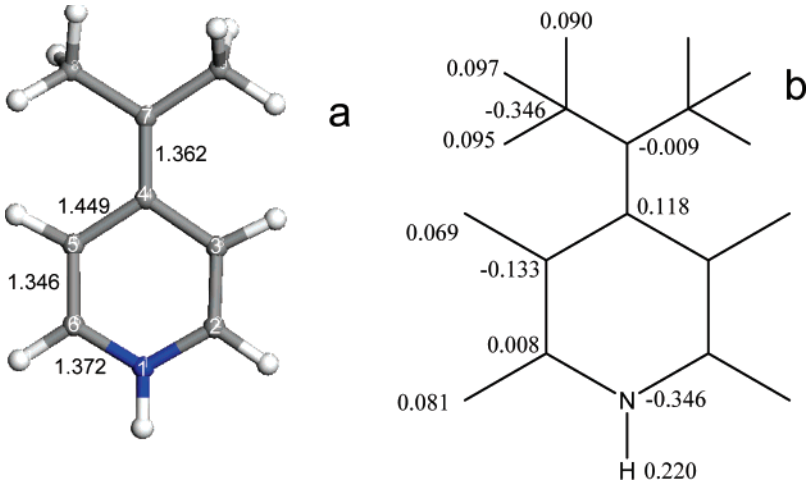

SCHEME 3: Modeling (DFT Level) of Electron Density Distribution in the Ground (HOMO) and Excited (LUMO) States of the Protonated Polymer Moiety[a]

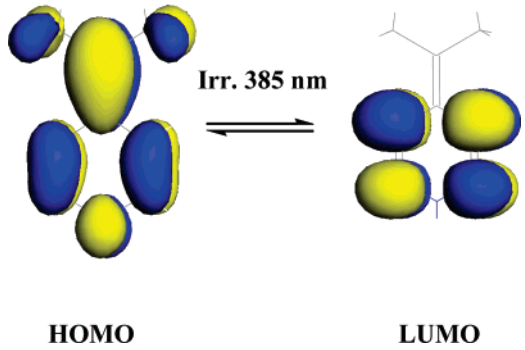

[a] Blue and yellow mark the negative and positive electron density, respectively.

off switching of the irradiating signal ($\sim$0.1−0.6 s^{-1}). g is the rate of absorption of the incident photons

$$g = \eta J/h\nu d \tag{3}$$

where J is the incident light flux (J = 5.3 mW/cm^2), $h\nu$ is the photon energy at 385 nm, d is the thickness of the gel layer (100 μm),[45] and η is the absorption probability of an incident photon. When the reflectivity of the gel is negligible and the absorption coefficient small, then the magnitude of the absorption probability of the incident photon can be shown to be equal to the optical density.[45] The optical density of the P4VPy gel at 385 nm in the presence of an electric field was 0.05. We used the photoinduced changes in resistance in both electrode arrangements (Figures 1 and 3) to calculate $\Delta\sigma$. We considered that in the conductivity measurements presented in Figure 1, the proton charge carriers dominate, while in the electrode arrangement of Figure 3, the electron conductivity dominates. We used $\sim 10^{-9}$ s as the value for τ_e, the lifetime of the charge carrier typical for electron transfer,[45] and for the proton, $\tau_p = \sim 35 \times 10^{-6}$ s.[44] Using eqs 2 and 3, the electron mobility in the gel was found to be $\sim$25 $cm^2\ V^{-1}\ s^{-1}$. This value is within the low range of electron mobilities in solid-state semiconductors.[44] In polymer semiconducting films,[46] the mobility is 0.1 $cm^2\ V^{-1}\ s^{-1}$. The proton mobility in the P4VPy gels was found to be $\sim 1.8 \times 10^{-3}$ $cm^2\ V^{-1}\ s^{-1}$. This value is within the range of proton mobilities found in ice.[47] Comparison of the time scales of the dark relaxation processes of the proton and electron components of the conductivity shows that the dark relaxation process is limited by proton transfer. The most reasonable explanation is the following: proton transfer is a directional process, and the presence of the hydrogen bonding retards it, while the electron conductance is a diffusion process in which the presence of hydrogen-bonded species can assist.

Modeling of Structure of Self-Protonated Polymer Pyridine Moiety in Ground and Excited States. Modeling of the optimal structure of the fully protonated polymer moieties R_{pol}CPy-H was performed using complete DFT geometric optimization (Module DMol^3, Accelrys)[30,31] (Scheme 2: (a) geometry (Å) and (b) Mulliken charge distribution). The molecule can clearly be identified as the cyclic structure of the polymeric pyridinium. The C2−C3 and C5−C6 bonds are significantly shorter than the other bonds; the charge distribution forms a weak electric dipole with μ = 2.93 D. The evaluation of the energies of the HOMO and LUMO of the singlet states gives −3.79 and −1.02 eV, respectively. The binding energy is 4.73 eV/atom, and the ionization potential is 6.27 eV (as compared to pyridine for which IP = 9.23 and 9.36 eV[48]). Ground-state conjugation around the ring (Scheme 3) influences (1) the electron conductive properties of the side-chain moiety and (2) the ability to build face-to-face complexes[49] with adjacent pyridine molecules, either free or bound.

Conclusion

We demonstrated that during the spontaneous gelation of the P4VPy/pyridine mixture, protonated and hydrogen-bonded structures on the polymer backbone were formed. Direct irradiation of the dielectric material (10^{-7} S/cm) at the proton-transfer center led to proton transfer and a decrease in the resistivity of the gel. The excited-state proton mobility was estimated to be $\sim 1.8 \times 10^{-3}$ $cm^2\ V^{-1}\ s^{-1}$. The proton-transfer channel may be viewed as an arrangement of protonated polymeric pyridine units in the excited state ($R_{pol}CPy^-$-H^+): $R_{pol}CPy^-$-$H^+\cdots R_{pol}CPy^-$-$H^+\cdots R_{pol}CPy^-$-$H^+\cdots R_{pol}CPy^-$-$H^+\cdots$, through which proton hopping can occur with or without the assistance of the free pyridine molecules. These interactions result in the bimolecular character of the conductivity. The interplay between the protonated, hydrogen-bonded pyridine side-chain units and the solvent molecules can act to form an intelligent structure with a diversity of possible functions, such as optical switching.

Acknowledgment. E.V. gratefully acknowledges financial support from the Israel Ministry for Immigrant Absorption. Fruitful discussions with the late Dr. L. Shapiro are greatly appreciated. This work was partly supported by the EC through contract FP6-029192.

References and Notes

(1) Vilkman, M.; Kosonen, H.; Nykanen, A.; Ruokolainen, J.; Torkkeli, M.; Serimaa, R.; Ikkala, O. *Macromolecules* **2005**, *38*, 7793−7791.
(2) Wei, Z.; Laitinen, T.; Smarsly, B.; Ikkala, O.; Faul, C. F. J. *Angew. Chem., Int. Ed*. **2005**, *44*, 751−756 (and references therein).
(3) Taylor, C. A.; El-Bayomi, M. A.; Kasha, M. *Proc. Natl. Acad. Sci. U.S.A.* **1969**, *63*, 253−260.
(4) Kreuer, K.-D. *Chem. Mater*. **1966**, *8*, 610−641.
(5) Ruokolainen, J.; Makinen, R.; Torkkeli, M.; Makela, T.; Serimaa, R.; Ten Brinke, G.; Ikkala, O. *Science (Washington, DC, U.S.)* **1998**, *280*, 557−560.
(6) Vikki, T.; Isotalo, H.; Ruokolainen, J.; Passiniemi, P.; Ikkala, O. *Synth. Met.* **1999**, *101*, 742−745.
(7) Ikkala, O.; Ten Brinke, G. *Science (Washington, DC, U.S.)* **2002**, *295*, 2407−2409.
(8) Guo, X.; Zhang, D.; Wan, G.; Yu, M.; Li, J.; Liu, Y.; Zhu, D. *Adv. Mater*. **2004**, *16*, 636−640.
(9) Förster, T. *Discuss. Faraday Soc*. **1959**, *27*, 7−17.
(10) Weller, A. *Prog. React. Kinet.* **1961**, *1*, 187−213.
(11) Tolbert, L. M.; Solntsev, K. M. *Acc. Chem. Res*. **2002**, *35*, 19−27 (and references therein).
(12) Solntsev, K. M.; Clower, C. E.; Tolbert, L. M.; Huppert, D. *J. Am. Chem. Soc*. **2005**, *127*, 8534−8544.
(13) Formosinho, S. J.; Arnaut, L. G. *J. Photochem. Photobiol., A* **1993**, *75*, 21−48.
(14) Douhal, A.; Lahmani, F.; Zewail, A. H. *Chem. Phys. Special Issue* **1996**, *207*, 477−498.
(15) Agmon, N. *J. Phys. Chem. A* **2005**, *109*, 13−35.
(16) Pang, X.-f.; Müller-Kirsten, H. J. W. *J. Phys.: Condens. Matter* **2000**, *12*, 885−906.
(17) Antonchenko, V. Y.; Davydov, A. S.; Zolotaryuk, A. V. *Phys. Status Solidi B* **1983**, *115*, 631−640.
(18) Leiderman, P.; Ben-Zvi, M.; Genosar, L.; Huppert, D.; Soltsev, K. M.; Tolbert, L. M. *J. Phys. Chem. B* **2004**, *108*, 8043−8053.
(19) Leiderman, P.; Huppert, D.; Agmon, N. *Biophys. J*. **2006**, *90*, 1009−1018.
(20) Lehtonen, O.; Hartikainen, J.; Rissanen, K.; Ikkala, O.; Pietilä, L.-O. *J. Chem. Phys*. **2002**, *116*, 2417−2424.
(21) Berkowitz, J. B.; Yamin, M.; Fuoss, R. M. *J. Polym. Sci*. **1958**, *28*, 69−82.
(22) Skapin, S.; Zupan, M.; Pejovnik, S. *Electrochim. Acta* **1997**, *42*, 2485−2492.
(23) Kabanov, V. A.; Evdakov, V. P.; Mustafaev, M. I.; Antipina, A. D. *Mol. Biol. (Moscow)* **1977**, *11*, 582−587.
(24) Pu, H. *Polym. Int*. **2003**, *52*, 1540−1545.
(25) Tiitu, M.; Torkkeli, M.; Serimaa, R.; Makela, T.; Ikkala, O. T. *Solid State Ionics* **2005**, *176*, 1291−1299.
(26) Uramoto, H.; Kawabata, N. *Electrochim. Acta* **1994**, *39*, 2181−2186.
(27) Rozenberg, M.; Vaganova, E.; Yitzchaik, S. *New J. Chem.* **2000**, *24*, 109−111.
(28) Vaganova, E.; Yitzchaik, S.; Shapiro, L.; Sigalov, M.; Khodorkovsky, V. *Adv. Mater*. **2000**, *12*, 1669−1671.
(29) Adamson, A. W. *A Textbook of Physical Chemistry*; Academic Press: San Diego, 1973; p 566.
(30) Delley, B. *J. Chem. Phys*. **1990**, *92*, 508−517.
(31) Delley, B. *J. Chem. Phys*. **2000**, *113*, 7756−7764.
(32) Perdew, J. P.; Burke, K.; Ernzerhof, M. *Phys. Rev. Lett.* **1996**, *77*, 3865−3868.
(33) Perdew, J. P.; Burke, K.; Ernzerhof, M. *Phys. Rev. Lett.* **1997**, *78*, 1396.
(34) Tabak, M. D.; Warter, P. J. *Phys. Rev*. **1966**, *148*, 982−990.
(35) Gurevitch, Y. Y.; Pleskov, Y. V.; Rotenberg, Z. A. *Photoelectrochemistry*; Consultants Bureau: New York, 1980; p 141.
(36) Chachisvilis, M.; Zewail, A. H. *J. Phys. Chem. A* **1999**, *103*, 7408−7418.
(37) Vaganova, E.; Meshulam, G.; Kotler, Z.; Rozenberg, M.; Yitzchaik, S. *J. Fluoresc*. **2000**, *10*, 81−88.
(38) Pierola, I. F.; Turro, N. J.; Kuo, P. L. *Macromolecules* **1989**, *18*, 508−511.
(39) Hägg, G. *General and Inorganic Chemistry*; Akmqvist and Wiksell Förlag AB: Stockholm, 1969; p 551.
(40) Vaganova, E.; Rozenberg, M.; Yitzchaik, S. *Chem. Mater*. **2000**, *12*, 261−263.
(41) Samoylova, E.; Smith, V. R.; Ritze, H.-H.; Radloff, W.; Kabelec, M.; Schultz, T. *J. Am. Chem. Soc*. **2005**, *128*, 15652−15656.
(42) Turro, N. J. *Molecular Photochemistry*; Benjamin, W. A., Inc., Advanced Book Program: Reading, MA, 1965; pp 85 and 150.
(43) Lakowicz, J. R. *Principles of Fluorescence Spectroscopy*; Kluwer Academic: Dordrecht, The Netherlands, 1999; p 128.
(44) Eigen, M.; De Mayer, L. *Proc. R. Soc. London, Ser. A* **1958**, *247*, 505−533.
(45) Petritz, R. L. *Phys. Rev*. **1956**, *104*, 1508−1516.
(46) Babel, A.; Jenekhe, S. A. *J. Am. Chem. Soc*. **2003**, *125*, 13656−13657.
(47) Kunst, M.; Warman, J. M. *Nature (London, U.K.)* **1980**, *288*, 466−467.
(48) Wan, J.; Hada, M.; Ehara, M.; Nakatasuji, H. *J. Chem. Phys*. **2001**, *114*, 5117−5123.
(49) Mishra, B. K.; Sathyamurthy, N. *J. Phys. Chem. A* **2005**, *109*, 6−8.